

Research on Dual-loop Controlled Grid-connected Inverters on the Basis of LCL Output Filters

Huichun Huang¹, Renjie Hu¹, Guiping Yi¹

¹*School of Electrical Engineering, Southeast University,
Sipailou RD. NO. 2, 210096 Nanjing, China
huanghuichun@seu.edu.cn*

Abstract—Under the premise that the same high-frequency filtering effect is realized, comparing with an L filter, an LCL filter, requiring less total inductance is more suitable for the application in grid-connected devices with low switching frequency and high power, but easier to cause current or voltage resonance and spike, thus further affecting the stability of the system. The design of the parameters not only influences the elimination effect of the ripple at the switching frequency, but also has impact on the operation performance of the devices. This paper establishes the mathematical models of inverter and LCL filter, adopts direct current dual-loop control strategy and analyses the stability, provides design analysis to LCL filter and gives the constraint and restriction conditions for the design of parameters. Moreover, this paper also carries out simulated research by means of Simulink and conducts experiments on the basis of the sample machine established. The result proves the correctness of the control strategy and design analysis herein.

Index Terms—Constraint and restriction condition, LCL filter, new control strategy, three-phase grid-connected inverter.

I. INTRODUCTION

With the extensive application of new-energy distributed power generation, grid connection technology has become an important research subject.

The traditional grid-connected inverter generally uses L filter to eliminate higher harmonics led in by switching device. However, in high-power inverter's applications, to reduce the loss and stress of the switching device, usually lower switching frequency is selected so as to increase the harmonic content in the grid-connected current. A higher inductance is required for the harmonic current to meet the same standard. The growth of the inductance value may cause a series of problems such as over large filter volume, current variation decrease and system performance reduction. With regards to this, substitution of LCL filter for L filter has become a trend in recent years. Comparing with L filter, LCL filter has better effect to eliminate higher harmonics, thus requires less inductance under certain harmonic elimination effect and shows more distinct advantages. In addition, the control technology based on LCL filter has also become one of new search focuses.

This paper establishes the mathematical models of inverter and LCL filter, puts forward direct current dual-loop control

strategy, provides design analysis to LCL filter and finally proves the correctness of the analysis herein through simulation and experiments. The design boasts high practical value in engineering.

II. ANALYSIS OF SYSTEM STRUCTURE AND MATHEMATICAL MODELS

A. System Structure

Figure 1 shows the main circuit topology of three-phase grid-connected inverter. Wherein, i_{ga} , i_{gb} and i_{gc} are the grid currents of the three phases, u_{ga} , u_{gb} and u_{gc} are the grid voltages of the three phases, i_a , i_b and i_c are the output currents of inverter, and the forward direction is as shown in the figure; grid inductance and its parasitic resistance are L_t and R_t respectively, inverter inductance and its parasitic resistance are L_f and R_f respectively, C_f is filtering capacitance; u_a , u_b and u_c are neutral-point voltage of inverter bridge, S_1 ~ S_6 are the power switching transistors of the IGBT, C is filtering capacitance of input DC side, U_{dc} is DC-side voltage, and L_t, L_f and C_f constitute the third-order LCL filter [1].

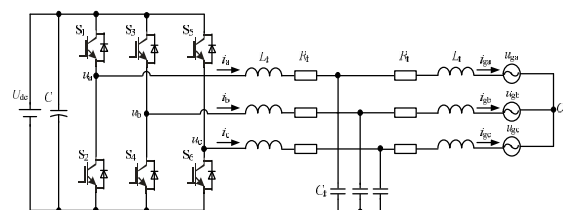


Fig. 1. Main circuit topology of three-phase grid-connected inverter.

Comparing with L filter, LCL filter has higher filtering capacitance C_f and filtering inductance L_t . The basic principle is as follows: L_t and C_f conducts shunting of the high-frequency ripple contained in L_f current i_f , and capacitance C_f provides low-impedance path for high-frequency current component generated by switch, which effectively reduces the high-frequency content of current i_t passing L_t . Therefore, LCL filter can be regarded as capacitance branch C_f connected with L_t branch in parallel, and then connected with L_f in series. i_t is capacitance branch C_f and L_t branch's shunting to L_f [2]–[6].

B. Mathematical Model of PWM Grid-Connected Inverter

For establishing the mathematical model of three-phase

grid-connected inverter by means of switching function, firstly define the switching function as follows

$$S_i = \begin{cases} 1 & (i_{\text{th}} \text{ switch ON}), \\ -1 & (i_{\text{th}} \text{ switch OFF}), \end{cases} \quad (1)$$

where $i = 1, 2, \dots, 6$.

$$\begin{cases} S_{ak} = \frac{1}{2} + \frac{1}{4}(S_1 - S_2), \\ S_{bk} = \frac{1}{2} + \frac{1}{4}(S_3 - S_4), \\ S_{ck} = \frac{1}{2} + \frac{1}{4}(S_5 - S_6), \end{cases} \quad (2)$$

where $k = 0, 1, \dots, 7$.

Let the neutral point of DC side be N, then the switching function from the output points a, b, c to the neutral point of DC side according to (1) and (2) can be obtained as:

$$\begin{cases} U_{aN} = S_{ak}U_{dc}, \\ U_{bN} = S_{bk}U_{dc}, \\ U_{cN} = S_{ck}U_{dc}, \end{cases} \quad (3)$$

where $k = 0, 1, \dots, 7$.

According to Fig. 1 and Kirchoff's Voltage Law, the below can be obtained:

$$\begin{cases} U_{aN} = U_{ao} + U_{oN}, \\ U_{bN} = U_{bo} + U_{oN}, \\ U_{cN} = U_{co} + U_{oN}. \end{cases} \quad (4)$$

If the voltage and load are three-phase symmetric, namely $U_{ao} + U_{bo} + U_{co} = 0$, then

$$U_{oN} = \frac{U_{aN} + U_{bN} + U_{cN}}{3}. \quad (5)$$

Based on an overall consideration of (1)–(5), the below can be obtained:

$$\begin{cases} U_{ao} = (2S_{ak} - S_{bk} - S_{ck})\frac{U_{dc}}{3}, \\ U_{bo} = (-S_{ak} + 2S_{bk} - S_{ck})\frac{U_{dc}}{3}, \\ U_{co} = (-S_{ak} - S_{bk} + 2S_{ck})\frac{U_{dc}}{3}. \end{cases} \quad (6)$$

C. Mathematical Model of LCL Filter

Figure 2 shows the single phase equivalent circuit and its block model of a LCL filter [7].

According to Fig. 2, the transfer function matrix of LCL filter by taking $U_k(s)$ and $U_{gk}(s)$ as the output quantity, $I_{gk}(s)$, $I_k(s)$ and $U_{ck}(s)$ as state quantity is as follows:

$$\begin{bmatrix} 0 & sL_f + R_f & 1 \\ sL_t + R_t & 0 & -1 \\ 1 & 1 & sC_f \end{bmatrix} \begin{bmatrix} I_{gk}(s) \\ I_k(s) \\ U_{ck}(s) \end{bmatrix} = \begin{bmatrix} U_k(s) \\ -U_{gk}(s) \\ 0 \end{bmatrix}, \quad (7)$$

where $U_{gk}(s)$ and $I_{gk}(s)$ are grid voltage and current respectively, $U_k(s)$ and $I_k(s)$ are voltage and current of bridge arm side, and $U_{ck}(s)$ is capacitor voltage. Make (1) be explicit function form, then

$$\begin{bmatrix} I_{gk}(s) \\ I_k(s) \\ U_{ck}(s) \end{bmatrix} = \frac{N(s)}{M(s)} \begin{bmatrix} U_k(s) \\ -U_{gk}(s) \\ 0 \end{bmatrix}, \quad (8)$$

where:

$$M(s) = L_t L_f C_f s^3 + (L_t R_f C_f + L_f R_t C_f) s^2 + (L_t + L_f + R_t R_f C_f) s + (R_t + R_f), \quad (9)$$

$$N(s) = \begin{bmatrix} 1 & C_f L_f s^2 + C_f R_f s + 1 \\ C_f L_t s^2 + C_f R_t s + 1 & 1 \\ L_t s + R_t & L_f s + R_f \end{bmatrix}. \quad (10)$$

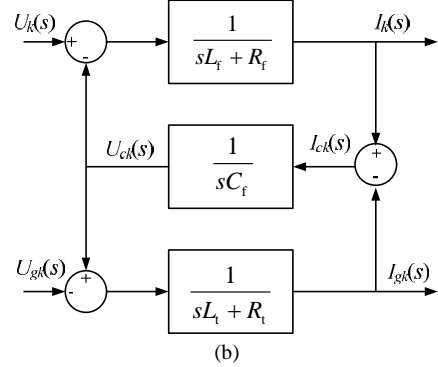
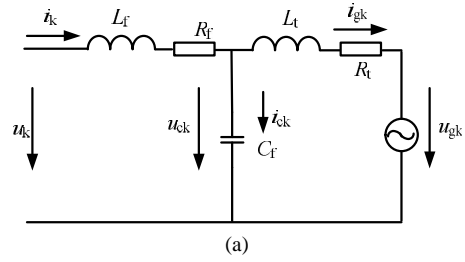


Fig. 2. Single phase equivalent circuit and its block model of a LCL filter: (a) single phase equivalent circuit, (b) block model.

III. CONTROL STRATEGY AND ITS STABILITY ANALYSIS

Figure 3 shows the block diagram of the principle structure of control strategy. The current feedback is unit feedback. Wherein, K is proportional control link; K_{PWM} is equivalent output gain of relative DC side of the inverter. The inductor current loop of the inverter side in Fig. 3(a) is used to protect the switching transistor and strengthen the system stability. The controller is a proportional controller and the coefficient is K . Figure 3(b) is the simplified block diagram of the structure obtained after equivalent conversion.

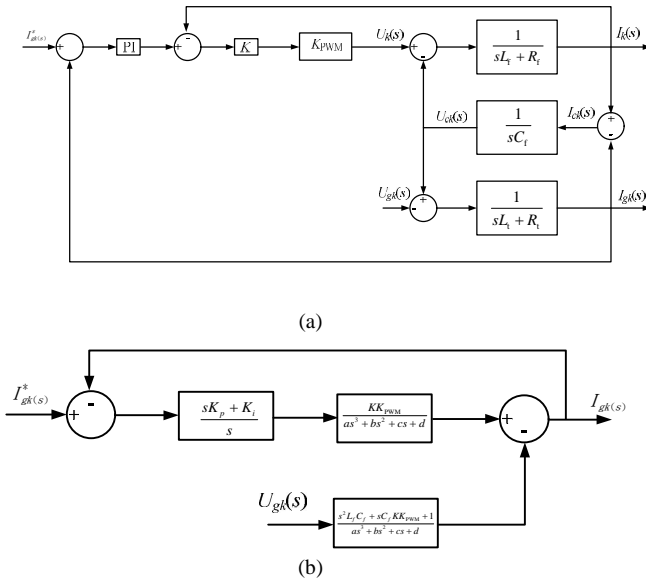


Fig. 3. Block diagram of direct grid-current controller with dual-loop: (a) Block diagram of the principle structure of control strategy, (b) Block diagram of the equivalent structure of control strategy.

In this way, the open-loop transfer function of the system is as follows [8]–[12]

$$G_1(s) = \frac{sK_p + K_i}{s} \cdot \frac{KK_{PWM}}{as^3 + bs^2 + cs + KK_{PWM}}. \quad (11)$$

To get the stability conditions of the system, the close-loop transfer function according to (3) can be as follows

$$G_2(s) = \frac{sK_p KK_{PWM} + K_i KK_{PWM}}{as^4 + bs^3 + cs^2 + ds + K_i KK_{PWM}}. \quad (12)$$

The characteristic equation of the close-loop transfer function is:

$$as^4 + bs^3 + cs^2 + ds + K_i KK_{PWM} = 0, \quad (13)$$

$$\begin{cases} a = L_t L_f C_f, \\ b = C_f (L_t R_f + L_f R_t + L_t KK_{PWM}), \\ c = R_t R_f + C_f R_t KK_{PWM} + L_t + L_f + R_t + R_f, \\ d = (K_p + 1) KK_{PWM}. \end{cases} \quad (14)$$

According to the Hurwitz stability criterion, the necessary and sufficient conditions of system stability include: all the coefficients in (5) more than zero, and:

$$\Delta_1 = KK_{PWM} L_t C_f > 0, \quad (15)$$

$$\Delta_2 = \begin{vmatrix} C_f (L_t R_f + L_f R_t + KK_{PWM} L_t) & (K_p + 1) KK_{PWM} \\ L_t L_f C_f & R_t R_f + R_t + R_f + L_t + L_f + C_f R_t KK_{PWM} \end{vmatrix} > 0, \quad (16)$$

$$\Delta_3 = \begin{vmatrix} C_f (L_t R_f + L_f R_t + KK_{PWM} L_t) & (K_p + 1) KK_{PWM} & 0 \\ L_t L_f C_f & R_t R_f + R_t + R_f + L_t + L_f + C_f R_t KK_{PWM} & K_i KK_{PWM} \\ 0 & C_f (L_t R_f + L_f R_t + KK_{PWM} L_t) & (K_p + 1) KK_{PWM} \end{vmatrix} > 0, \quad (17)$$

$$\Delta_4 = K_i KK_{PWM} \Delta_3 > 0. \quad (18)$$

According to (15)–(18), the boundary values of K_i , K_p can be obtained.

IV. DESIGN AND ANALYSIS OF LCL FILTER

A. Requirements for parameters design for the filter

Under the premise of saving total inductance materials as far as possible, the LCL filter with optimum performance is designed and the following constraint conditions shall also be satisfied [13]–[15]:

To shunt the ripple current component of switch frequency and let the high-frequency component pass through capacitor branch if possible, the condition of $X_{Cf} \ll X_{Lt}$ shall be met during design, wherein X_{Cf} and X_{Lt} are impedance values under switch frequency, and take

$$X_{Cf} = \left(\frac{1}{10} \sim \frac{1}{5} \right) X_{Lt}. \quad (19)$$

When X_{Cf} value is too small, the filtering capacitance value will be high, and the reactive current flowing through the filtering capacitance will be more, as a result the output current of the inverter is increased and the loss is increased accordingly. When X_{Cf} value is too big, the filtering capacitance value will be low, and the ripple high-frequency

component of capacitor branch will be insufficient, as a result the high-frequency harmonic current component flows into the grid. Moreover, to prevent over low of the power factor of the grid-connected inverter, it is required that the fundamental reactive power absorbed by filtering capacitance is no more than 5 % of the rated active power of the system. Thus

$$C_f \leq \frac{\} p}{3 \times 2f f_b u_g^2}, \quad (20)$$

where P is the rated output active power of grid-connected inverter; $\}$ is the proportion of fundamental reactive power absorbed by filtering capacitance in P ; u_g is the valid value of grid phase voltage.

The impedance drop on LCL filter's inductance is less than 10 % of the rated working voltage of the grid.

The resonance point existent in the LCL filter may lead to oscillation and distortion of grid-connected current, and even affect the inverter's stability. To avoid the influences of the resonance point on the system, it is required to limit the value-taking range of resonance frequency f_{res}

$$f_{res} = \frac{1}{2f} \sqrt{\frac{L_t + L_f}{L_t L_f C_f}}. \quad (21)$$

Generally, f_{res} is set to be more than 10 times of grid frequency and less than 1/2 of switch frequency

$$10f_b \leq f_{res} \leq \frac{1}{2}f_s, \quad (22)$$

where f_s is the switch frequency of the inverter, f_b is the grid fundamental frequency, and the harmonics in this range is relatively few.

B. Parameters Design for the LCL Filter

The specific parameters are as follows: the rated capacity of the three-phase grid-connected inverter $P_n = 40$ kVA, grid voltage is $u_g = 220$ V, switch frequency $f_s = 6$ kHz, and voltage of DC side $U_{dc} = 800$ V [16]–[21].

Design of filtering capacitance. The reactive power absorbed by filtering capacitance C_f is generally less than 5%. Taking 3% herein, the below can be obtained

$$C_f = 3\% \times \frac{P_n}{3 \times 2f f_b u_g^2}. \quad (23)$$

Upon calculation, we can get the result $C_f = 13.5$ μ F.

Design of the inductance of inverter side. The design method of the inductance of inverter side L_f can refer to the traditional single L filter. The inductance drop of filter is no more than 10% of the voltage (r.m.s) of the grid line, the current ripple is usually limited to 10%–25%, take 16% herein, namely:

$$\Delta i = \frac{U_{dc}}{7L_f f_s} \leq 16\% I_n, \quad (24)$$

where Δi is ripple current and I_n is rated current. According to the parameters design conditions, the minimum value of L_f is: $L_f = 0.7$ mH.

Design of the inductance of grid side. The relationship between the inverter-side inductance and the grid-side inductance is

$$L_t = rL_f. \quad (25)$$

The current ripple decay caused by LCL filter is

$$\frac{i_m(h)}{i(h)} = \frac{1}{|1 + r[1 - (2f f_s)^2 L_f C_f]|}, \quad (26)$$

where $i(h)$, $i_m(h)$ is the current harmonic of inverter side and the grid current harmonic of switch frequency respectively. The relationship curve between the ripple current decay of switch frequency and r is as shown in Fig. 4. Take $r = 0.6$, then the ripple current decay is 5%, $L_t = 1.13$ mH.

V. SIMULATION AND EXPERIMENTAL RESEARCH

A. Simulated Analysis of three-phase grid-connected inverter

To demonstrate the correctness and feasibility of the

parameters' design and control strategy in this paper, a simulation model of the three-phase grid-connected inverter with LCL filter is established in Simulink for simulation and research. The simulation parameters are: three-phase grid line voltage – 380 V, grid frequency – 50 Hz, switch frequency – 6 kHz, inductance of AC side $L_t = 1.13$ mH, inductance of inverter side $L_f = 0.7$ mH, and filtering capacitance $C_f = 13.5$ μ F.

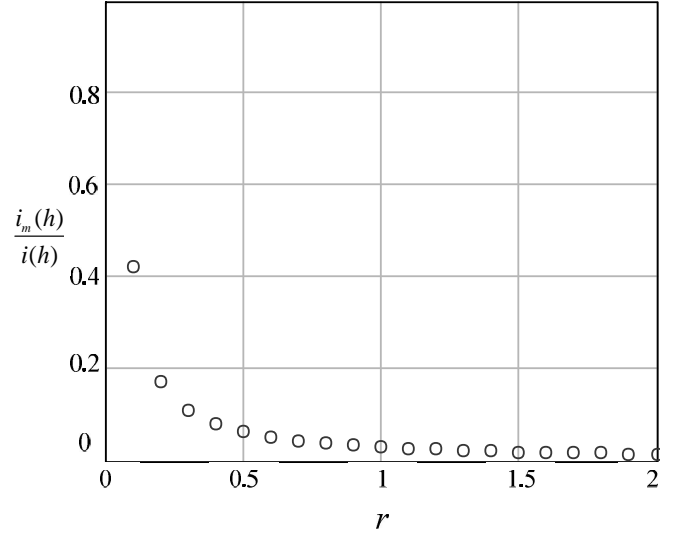


Fig. 4. The relationship curve between the ripple current decay of switch frequency and r .

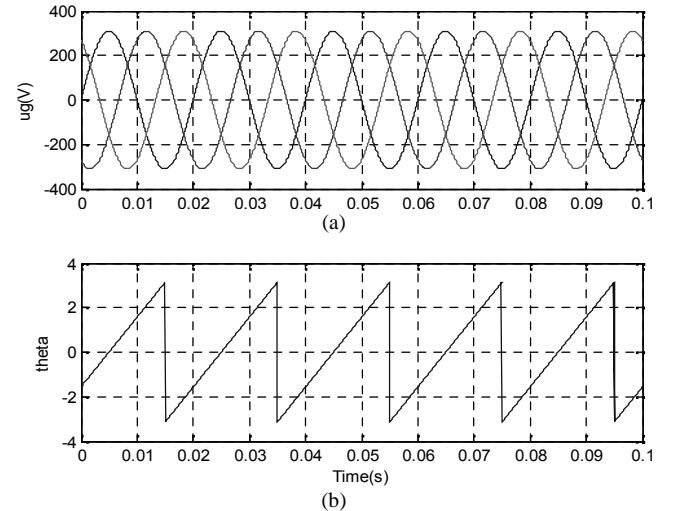
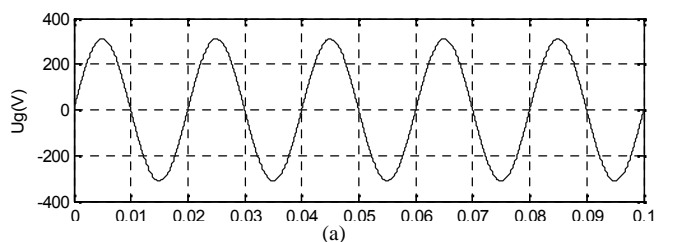


Fig. 5. The voltage and phase-locked angle waveforms of three-phase power grid.

Figure 5 shows the voltage and phase-locked angle waveforms of three-phase power grid. According to the figure, the phase-locked angle ranges from - to , between the peak and the valley of the grid voltage and the frequency is 50 Hz.



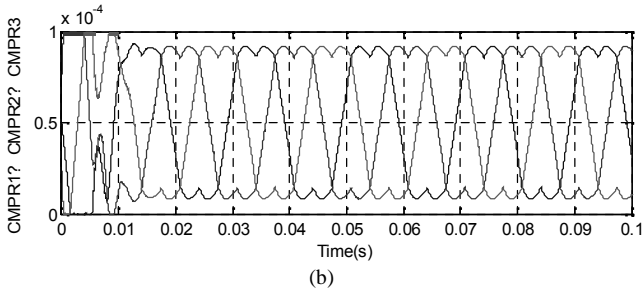


Fig. 6. The waveforms of grid voltage of phase A and three-phase modulation waves.

Figure 6 shows the waveforms of grid voltage of phase A and modulation waves CMR1, CMR2 and CMR3. According to the figure, the modulation waveforms are saddle type, which can effectively improve the utilization rate of SC side voltage. The voltage frequency of CMR1 is the same as that of the neutral point of phase A bridge arm, but the phases are opposite.

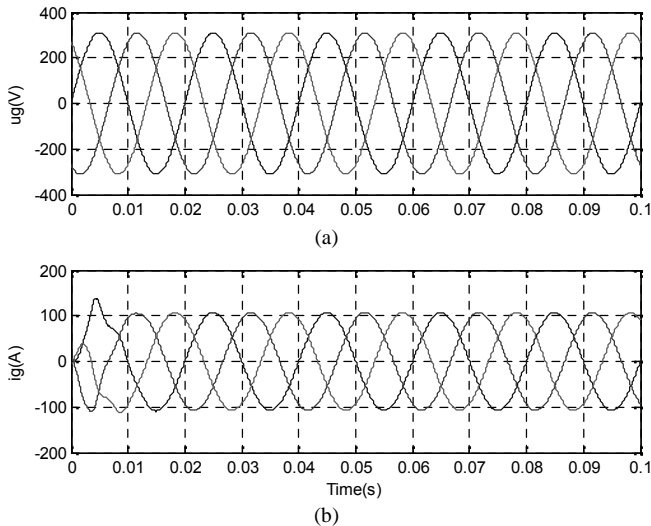


Fig. 7. The waveforms of three-phase grid voltage and current with full-load LCL filter.

Figure 7 shows the waveforms of three-phase grid voltage and current with full-load three-phase grid-connected LCL filter. Figure 8(a) shows the grid harmonic current spectrum analysis. The current at this time mainly includes fundamental wave and its frequency multiplication component, and switch frequency component. Figure 8(b) shows the inverter-side harmonic current spectrum analysis. The current at this time mainly includes fundamental wave and its frequency multiplication component, switch frequency and its frequency multiplication component. Figure 8(c) shows the harmonic current spectrum analysis of filtering capacitance branch. The current at this time mainly includes switch frequency and its frequency multiplication component.

B. Experimental Research

To further demonstrate the correctness of the analysis in this paper, an LCL filter grid-connected inverter prototype with TMS320 LF2812 as the core processor is established for experimental research. The main experimental parameters are as shown in Table I.

Figure 9 shows the voltage and phase locked angle experimental waveforms of three-phase power grid. Figure 10 shows the experimental waveforms of grid voltage of phase A

and three-phase modulation waves. Figure 11 shows the experimental waveforms with full load.

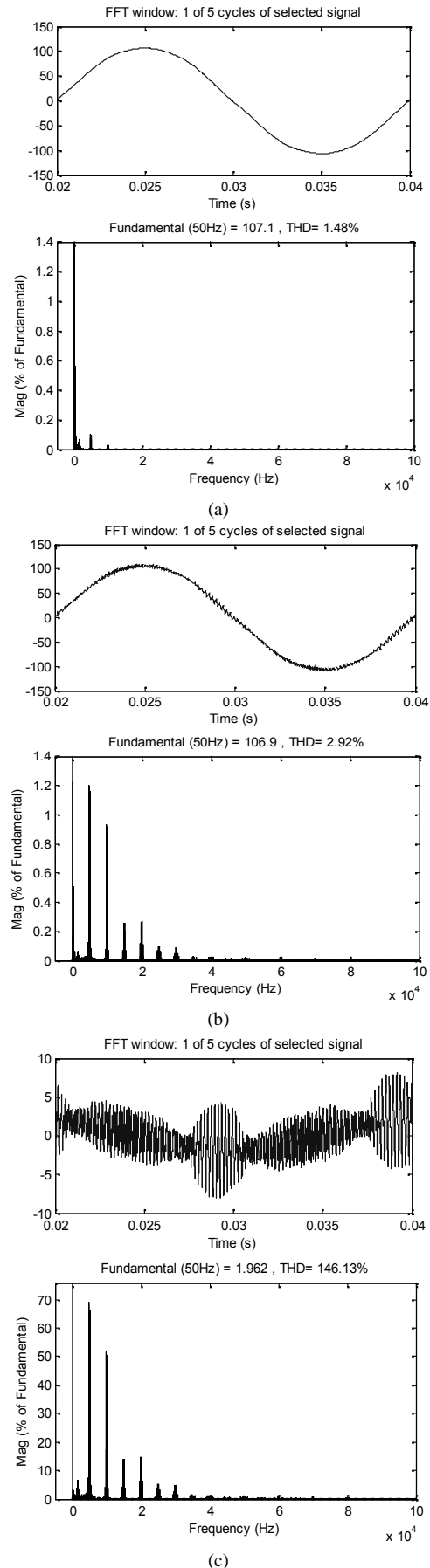


Fig. 8. Current harmonic analysis; (a) grid current harmonic analysis, (b) inverter current harmonic analysis, (c) current harmonic analysis of filtering capacitance branch.

TABLE I. PARAMETER AND ITS VALUE.

Paramete	value
Input DC voltage U_{dc}	800 V
Grid phase voltage U_g	220 V/50 Hz
Switch frequency f_s	6 kHz
Rated power P_n	40 kVA
Inductance of inverter side L_f	0.7 mH
Grid inductance L_t	1.13 mH
Filtering capacitance C_f	13.5 μ F

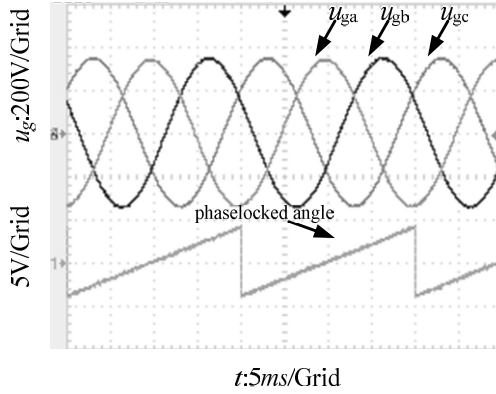


Fig. 9. The voltage and phaselocked angle waveforms of three-phase power grid.

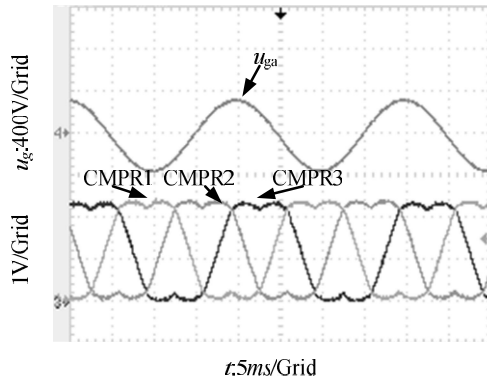


Fig. 10. The waveforms of grid voltage of phase A and three-phase modulation waves.

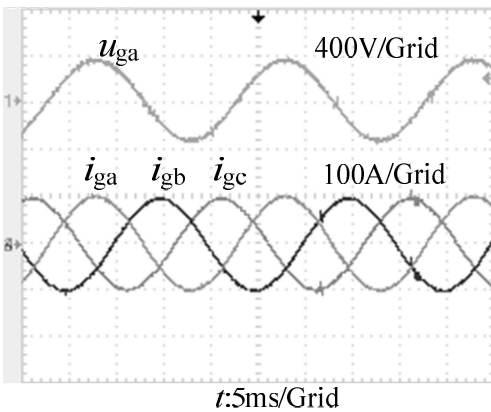


Fig. 11. The experimental waveforms with full load.

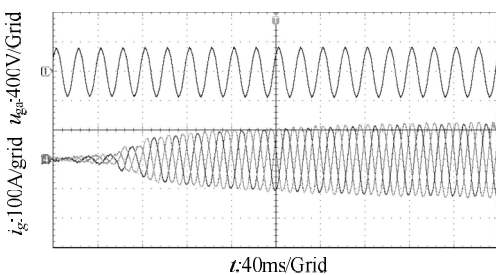


Fig. 12. Sudden load process.

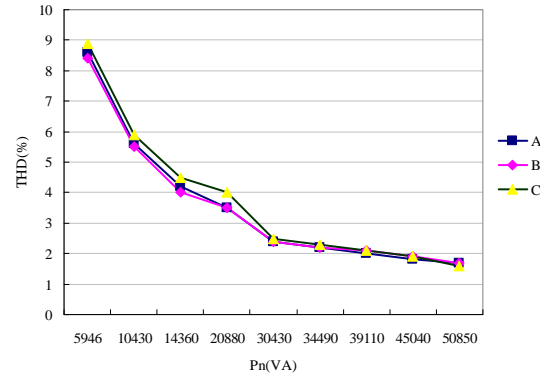


Fig. 13. The THD curve of grid current with the input power changing.

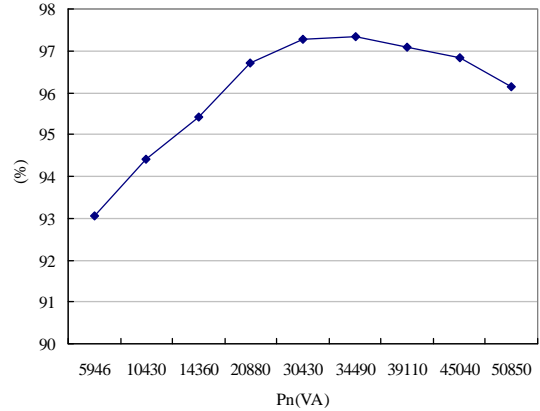


Fig. 14. System efficiency curve.

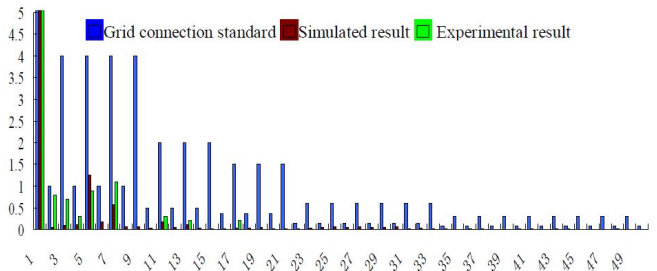


Fig. 15. Grid current harmonic analysis and comparison.

Figure 12 shows the sudden load process from no load to full load of the system. According to the figure, there are about 20 power frequency cycles from no load to full load, realizing lazy load. Figure 13 shows the THD curve of grid current with the input power changing. It can be concluded from the figure that, when the grid power is increased, the THD of current is decreased accordingly. Figure 14 shows the system prototype's efficiency curve. From the curve, we can see that the system efficiency is above 93 %, and the efficiency near full load is above 97 %. Figure 15 is a bar chart showing the grid current harmonic analysis and comparison of grid-connected standard, simulated and experimental conditions. It can be concluded from the figure that the system fully satisfies the grid-connected requirements.

VI. CONCLUSIONS

This paper establishes the mathematical models of grid-connected inverter and LCL filter, puts forward direct current dual-loop control strategy, provides design analysis to LCL filter on the basis of the limitation conditions of the

design parameters introduced, realizes grid-connected operation of grid current direct control by means of the experimental platform of grid-connected inverter finally and proves the correctness and effectiveness of the parameters design solution based on direct current control strategy.

REFERENCES

- [1] Lin Weixun, *Modern Power Electronics*. Beijing: China Machine Press, 2006, pp. 3–4.
- [2] A. N. Celik, “Present status of photovoltaic energy in Turkey and life cycle techno-economic analysis of a grid-connected photovoltaic-house”, *Renewable & Sustainable Energy Reviews*, vol. 10, no. 4, pp. 370–387, 2006. [Online]. Available: <http://dx.doi.org/10.1016/j.rser.2004.09.007>
- [3] K. A. Nigim, A. F. Zobaa, “Development and opportunities of distributed generation fueled by renewable energy sources”, *Int. Journal of Global Energy Issues*, vol. 26, no. 3–4, pp. 215–231, 2006. [Online]. Available: <http://dx.doi.org/10.1504/IJGEI.2006.011257>
- [4] K. Sire, C. Q. Lee, T. F. Wu, “Current distribution control for parallel connected converter: Part 2”, *IEEE Trans. Aerospace and Electronic Systems*, vol. 28, no. 3, pp. 841–850, 1992. [Online]. Available: <http://dx.doi.org/10.1109/7.256304>
- [5] T. Erika, G. H. Donald, “Grid current regulation of a three-phase voltage source inverter with an LCL input filter”, *IEEE Trans. Power Electronics*, vol. 18, no. 3, pp. 888–895, 2003. [Online]. Available: <http://dx.doi.org/10.1109/TPEL.2003.810838>
- [6] Y. Chen, F. Liu, “Design and control for three-phase grid-connected photovoltaic inverter with LCL filter”, in *IEEE Circuit and Systems Int. Conf. on Digital Object Identifier*, 2009, pp. 1–4.
- [7] Guo Xiaoqiang, Wu Weiyang, Gu Herong, et al. “Modelling and stability Analysis of direct output current control for LCL interfaced grid-connected inverters”, *Trans. of China Electrotechnical Society*, vol. 25, no. 3, pp. 102–109, 2010.
- [8] E. Wu, P. W. Lehn, “Digital current control of a voltage source converter with active damping of LCL resonance”, *IEEE Trans. Power Electronics*, vol. 21, no. 5, pp. 1364–1373, 2006. [Online]. Available: <http://dx.doi.org/10.1109/TPEL.2006.880271>
- [9] Shen Guoqiao, Xu Dehong, Xi Danji, et al., “An improved control strategy for grid-connected voltage source inverters with a LCL filter”, in *21th Annual IEEE Applied Power Electronics Conf. and Exposition (APEC 06)*, 2006, pp. 1067–1073.
- [10] Wen Feng, Jia Guanghui, *Automatic control theory*, Beijing: China Electric Power Press, 2002.
- [11] B. Halimi, P. A. Dahono, “A current control method for phase-controlled rectifier that has an LCL filter”, in *Proc. 4th IEEE Int. Conf.*, 2001, pp. 20–25.
- [12] Zhao Qinglin, Guo Xiaoqiang, Wu Weiyang. “Research on control strategy for single-phase grid-connected inverter”, in *Proc. CSEE*, 2007, vol. 27, no. 16, pp. 60–64.
- [13] P. C. Loh, “Analysis of multiloop control strategies for LC/CL/LCL filtered voltage-source and current-source inverters”, *IEEE Trans. Industry Applications*, vol. 41, pp. 644–654, 2005. [Online]. Available: <http://dx.doi.org/10.1109/TIA.2005.844860>
- [14] Wu Weimin, Liu Songpei, He Yuanbin, et al. “Overview of current control technique for single-phase grid-connected inverter with LCL filter”, *Journal of Power Supply*, vol. 2, pp. 51–58, 2011.
- [15] Wu Jiaju, Zhang Chaoyan, Ren Jilin, et al. “A method for designing non-symmetry T-network filter used in PWM inverters”, in *Proc. CSEE*, 2005, vol. 25, no. 14, pp. 35–40.
- [16] Dong Mi, Luo An, “Design and control strategies of inverter for a grid-connected photovoltaic power system”, *Automation of Electric Power System*, vol. 30, no. 20, pp. 97–102, 2006.
- [17] M. Liserre, F. Blaabjerg, S. Hansen, “Design and control of an LCL-filter based three-phase active rectifier”, in *36th IAS Annual Meeting Conf. Record of the IEEE*, 2001, vol. 1, pp. 299–307.
- [18] Wang Zhengshi, Chen Huiming, “Design of grid-tied inverters with the functions of reactive and harmonic compensation”, *Automation of Electric Power System*, vol. 31, no. 13, pp. 67–71, 2007.
- [19] Lang Yongqiang, Xu Dianguo, Hadianamrei SR, et al. “A novel design method of LCL type utility interface for three-phase voltage source rectifier”, in *IEEE Power Electronics Specialists Conf.*, Recife, Brazil, 2006.
- [20] Zhang Xianping, Li Yaxi, Pan Lei, et al. “Analysis and design of LCL type filter for three-phase voltage source rectifier”, *Electrotechnical Application*, vol. 26, no. 5, pp. 65–67, 2007.
- [21] Sun Shaohua, Li Chunpeng, Ben Hongqi, “Design of three-phase grid-connected inverter with LCL filter”, *Trans. of China Electrotechnical Society*, vol. 26, no. 1, pp. 107–112, 2011.